AAPS PharmSciTech, Vol. 10, No. 3, September 2009 (© 2009)
DOI: 10.1208/s12249-009-9296-0

Research Article

Formulation of Dacarbazine-loaded Cubosomes—Part II: Influence of Process Parameters

Di Bei,[1] Jacob Marszalek,[2] and Bi-Botti C. Youan[1,3]

Received 5 March 2009; accepted 27 July 2009; published online 18 August 2009

Abstract. The purpose of this study is to investigate the combined influence of process parameters (independent variables) such as homogenization speed (X_1), duration (X_2), and temperature (X_3) during the preparation of dacarbazine-loaded cubosomes. Box–Behnken design was used to rationalize the influence of these three factors on two responses, namely particle size (Y_1) and encapsulation efficiency (Y_2). Independent and dependent variables were analyzed with multiple regressions to establish a full-model second-order polynomial equation. *F* value was calculated to confirm the omission of insignificant parameters or interactions of parameters from the analysis to derive a reduced-model polynomial equation to predict the Y_1 and Y_2 of dacarbazine-loaded cubosomes. Pareto charts were also obtained to show the effects of X_1, X_2, and X_3 on Y_1 and Y_2. For Y_1, there was a model validated for more accurate prediction of response parameter by performing checkpoint analysis. The optimization process and Pareto charts were obtained automatically and they predicted the levels of independent parameters X_1, X_2, and X_3 (0.889794, 0.11886, and 0.56201, respectively) and minimized Y_1. The optimal process parameters (homogenization's speed=~24,000 rpm, duration=5.5 min, and temperature=76°C) led to the production of cubosomes with 85.6 nm in size and 16.7% in encapsulation efficiency. The Box–Behnken design proved to be a useful tool in the preparation and optimization of dacarbazine-loaded cubosomes. For encapsulation efficiency (Y_2), further studies are needed to enhance the result and improve the model for such water-soluble drug encapsulation in cubosomes.

KEY WORDS: Box–Behnken design; cubosomes; dacarbazine; optimization; process.

INTRODUCTION

In the late 1960s, the bicontinuous liquid crystal phase was first reported (1) and its geometric model was later provided in the mid-1970s (2). Among these types of phase, cubosomes, especially made of binary systems, and monoolein–water (3) are one of the most studied. Due to emerging interest in pharmaceutical nanotechnology, there have been several investigations on the use of these systems as alternative drug delivery systems. Thus, they have been investigated for different pharmaceutical applications (peptides, enzymes, antimuscarinic drugs, antibiotics, analgesic delivery) and extensively reviewed (4–10).

The promise for these liquid crystals is found in their unique bicontinuous liquid crystal structure. These systems are interesting nanocarriers for drug delivery because of: (1) their three-dimensional network or "honeycombed" structure (11) separating two identical water channels with a pore diameter of about 5 nm in the fully hydrated state (8,12) and large internal surface area (~400 m^2/g) (13) that may allow high drug loading and controlled drug delivery; (2) their protective properties of the biodegradable lipid/water matrix; (3) their potential ability to incorporate and slowly release drugs with different physicochemical properties (amphiphile, hydrophilic, and hydrophobic) into the tightly packed "honeycombed" structure with bicontinuous domains of water and lipid (11); (4) they are potentially syringeable and thus may be easier to administer than the very viscous cubic phase particularly for parenteral administration (8,14,15); and (5) their potential to overcome the stability and drug loading/broad applicabilities issues related to other drug nanocarriers such as liposomes (11). Moreover, specifically for this project, it is hypothesized that the transdermal transport of the encapsulated drug may be enhanced based on recent findings on the similarities between the bicontinuous structures formed in human skin bilayers and those comprising cubosomes (16).

Different methods have been used to prepare colloidal monoglyceride dispersions (10). They are either based on fragmentation using high-energy devices (17) or precipitation techniques involving the formation of colloidal particles upon dilution of the solutions of the monoglyceride (18). It is increasingly recognized that there is a knowledge gap on the formulation of cubosomes for pharmaceutical applications with respect to formulation variable and process parameters in order to maximize transformation to the cubic phase while

[1] Division of Pharmaceutical Sciences, University of Missouri—Kansas City School of Pharmacy, Room# 108E, 5005 Rockhill Road, Kansas City, Missouri 64110-2499, USA.
[2] Division of Counseling and Education Psychology, University of Missouri—Kansas City School of Education, 5100 Rockhill Road, Kansas City, Missouri 64110-2499, USA.
[3] To whom correspondence should be addressed. (e-mail: youanb@umkc.edu)

avoiding aggregation during formulation (10) and also enhanced drug entrapment.

Dacarbazine (DTIC), a water-soluble drug, is currently used as a first line chemotherapy medication against melanoma (19). In our previous report (20), we investigated the influence of formulation variables of dacarbazine-loaded cubosomes. To contribute to the knowledge gap in cubosome formulation, the current study is an extension of our previous one with special emphasis on the influence of process parameters.

Since the first formulation of cubosomes, scientists have performed research on their physicochemical properties (7,21), their physiological behavior (15), and their interactions with other substances (22). Some researchers have investigated the phase behavior of monoolein/poloxamer/water during the preparation of cubosomes (8–10,18). However, the phase behavior of homogenization speed/duration/temperature was seldom studied. Moreover, there is emerging interest in using statistical methods to optimize pharmaceutical formulations (23–25). However, to our knowledge, such methods have seldom been used specifically for drug-loaded cubosome formulation. To contribute to bridging the knowledge gap, the experiments in this study are designed to assess the influence of process parameters including homogenization speed, duration, and temperature upon cubosome preparation by an adapted fragmentation technique.

MATERIALS AND METHODS

The glycerol monooleate RYLO MG 19 (MO) was a gift from Danisco Cultor (Grindsted, Denmark). Poloxamer 407 (Pluronic F127) was a gift from BASF Corporation (Ludwigshafen, Germany). Phosphate buffer saline (PBS) and dacarbazine (DTIC) were purchased from Sigma Aldrich (St. Louis, MO, USA). Chloroform was purchased from Fisher Scientific (Pittsburgh, PA, USA). All chemicals used in the study were of analytical grade and used without further purification.

Box–Behnken Experimental Design

A Box–Behnken statistical design (26) with three levels, three factors, and 15 runs of experiments was selected for our study for the purpose of optimization. The independent and dependent parameters are listed in Table I. The polynomial equation was as follows:

$$Y_i = b_0 + b_1X_1 + b_2X_2 + b_3X_3 + b_{12}X_1X_2 + b_{13}X_1X_3 + b_{23}X_2X_3 + b_{11}{X_1}^2 + b_{22}{X_2}^2 + b_{33}{X_3}^2 \quad (1)$$

where Y_i is the dependent variable; b_0 is the intercept with Y-axis; b_1 to b_{33} are the regression coefficients; and X_1, X_2, and X_3 are the coded independent variables that were selected based on the preliminary experiments. The preliminary data indicated in this context referred specifically to previous literature works related to cubosomes preparation methods underlined in the INTRODUCTION. The main objective here was to focus on the experimental design aspects based on these previous literature works. Basically, before starting this experimental design, several samples were prepared not only for feasibility study but also to identify the relevant process parameters and their acceptable lowest and upper limits based on the operating conditions.

Table I. Independent Variables and their Levels in Box–Behnken Design

	Low	Medium	High
Independent variables			
X_1: homogenization speed (rpm)	6,500	13,500	24,000
X_2: duration (min)	1	5	9
X_3: temperature (°C)	60	70	80
Coded values	−1	0	1
Dependent variables			
Y_1=particle size (nm)			
Y_2=encapsulation efficiency (EE)			

In this study, the three key process variables (homogenization speed, duration, and temperature) were represented by X_1, X_2, and X_3, respectively, because cubosomes preparation process is an energy-dependent process (7).

Preparation of Dacarbazine-Loaded Cubosomes

The method of preparation of dacarbazine-loaded cubosomes were adapted from of work of Esposito *et al.* (17). Briefly, for each sample, a volume of 15 ml chloroform was used to completely dissolve 500 mg MO and Pluronic F127 75 mg. All the 15 runs of experiments were prepared according to the Box–Behnken design in Table II. The flask was then attached to a rotavapor to evaporate chloroform at 60 rpm, at a temperature of 60±2°C. Then, after evaporation, there was a thin film formed at the bottom of the flask. A volume of 50 ml of PBS (pH=7.4) was used to dissolve 2 mg of water-soluble dacarbazine and then this solution was added into the dry lipid film to form coarse dispersions. A sonicator was used to briefly mix the lipid film and water phase together. This coarse dispersion was then kept at the desired temperature for 15 min in a water bath. Then, we transferred the hot mixture swiftly to a beaker in which a homogenizer (IKA ULTRA-TURRAX T-25, Staufen, Germany) was used to prepare uniform dispersion. Cubosomes were formed when the dispersion cooled down to room temperature gradually. Aluminum coils were used to cover the sample vials in order to protect samples from direct light. The dispersions were then used for future tests and evaluation.

Particle Size Determination

The particle size of the cubosomes was determined through dynamic light scattering (DLS, Brookhaven Instruments Corporation, Austin, TX, USA). DLS, sometimes referred to as photon correlation spectroscopy, is a non-invasive, well-established technique for measuring the size of molecules and particles typically in the submicron region. The measurements were taken under a temperature of 25°C, a laser wavelength of 659.0 nm, and a refractive index of 1.330. The samples were vortexed before measuring the particle size. In this study, particle size and size distribution (polydispersity) of cubosome samples were measured. The samples were vortexed before measuring the mean diameter and size

Table II. Box–Behnken Experimental Design of Independent Variables with Measured Responses

Run no.	X_1	X_2	X_3	Y_1	PI	Y_2 (%)
1	0	0	0	107	0.103	29.4
2	1	0	1	93.9	0.127	7.3
3	0	0	0	107	0.130	23.0
4	−1	1	0	144.9	0.005	28.4
5	1	−1	0	106.8	0.021	9.1
6	−1	−1	0	252.2	0.005	13.1
7	1	1	0	96.5	0.154	26.1
8	0	−1	−1	149.2	0.005	33.8
9	−1	0	1	200.8	0.005	7.0
10	0	1	1	112.9	0.076	7.8
11	0	1	−1	110.6	0.187	14.4
12	0	0	0	123.0	0.081	9.1
13	−1	0	−1	139.9	0.005	4.6
14	0	−1	1	163.7	0.005	30.0
15	1	0	−1	88.2	0.191	25.1

Y_1 mean diameter, *PI* polydispersity index, Y_2 percent encapsulation efficiency

distribution and polydispersity of cubosomes. Based on National Institute Standard, a PI<0.05 was considered monodispersed (27).

Transmission Electron Microscopy (TEM)

The samples were prepared by putting a 5-μl droplet of the cubosome suspension onto a 300 mesh carbon-coated copper grid, and letting the cubosomes settle for 3–5 min. Then, the excess fluid was removed by wicking it off with an absorbent paper. The samples were negatively stained in 1% uranyl acetate for 3–5 min. The samples were then viewed on a JEOL Model JEM 1400 120 kV transmission electron microscope (JEOL, Wilmington, DE, USA) and photographed digitally on a Gatan axis-mount 2k×2k digital camera.

Encapsulation Efficiency

The encapsulation efficiency (Y_2) was measured at the wavelength of 330 nm with a UV spectrometer (NanoDrop Model 1000, Thermo Fisher Scientific, DE, USA). This spectrometer enables highly accurate UV/Vis analyses of 1-μl samples with remarkable reproducibility. The standard curve, based on the dacarbazine concentration from 0 to 360μg/ml, had a regression equation of $y=0.0061x-0.0081$ with R^2 of 0.9985. In this study, all UV measurements and calculations of Y_2 were based on this specific equipment and standard curve. In all 15 runs of experiments, the measurement of EE was carried out with one specific kind of centrifuge tube, Amicon Ultra 3,000 MWCO (Millipore, USA). Preliminary studies conducted with known concentrations of drug from the calibration curve showed that this specific drug did not significantly bind to the membrane Ultra 3,000. Moreover, the UV molar absorptivity (ε ~11,200 l/mol cm) did not change significantly for free and uncapsulated drug. In each experiment, after the sample cooled down to room temperature, it was transferred to the centrifuge tubes and put to 1,500 rpm for 30 min. Non-encapsulated drug or free drug in solution leaked outside the sub-tubes, making it possible to measure its concentration in solution, and thus allowed the deduction of the drug encapsulated in cubosomes. That UV absorbance was used to compute C_t (namely, total concentration) and the UV absorbance of dacarbazine contained in filtrate after centrifuge was used to compute C_f (namely, filtrate concentration). Thus, the encapsulation efficiency was calculated as follows:

$$EE\% = \left[\left(C_t - C_f\right)/C_t\right] \times 100 \quad (2)$$

Master Formula

Polynomial equations of the response values Y_1 and Y_2 for three-level, three-factor parameters were developed after the interpretation of data (Eqs. 4 and 5, respectively). Since the polynomial equations for Y_1 fit well (R^2=0.974, adj. R^2= 0.972; 0.90 is considered acceptable fit), they were used for optimization. Since the polynomial equation for Y_2 did not fit well (R^2=0.76, adj. R^2=0.328), it was not appropriate for further analysis and interpretation. Because nanoparticles with smaller size have a greater potential for permeability, cellular and tissue targeting ability, the optimization was performed towards minimizing particle size (Y_1) based on the three levels of independent parameters (X_1, X_2, and X_3).

Checkpoint Analysis

After deleting irrelevant parameters and interactions from the initial equation, a checkpoint analysis was performed to make more sense of the analysis of the secondary (reduced) equation, which was very useful in optimizing and predicting the responses. Three points were selected: two random points (−0.5, −0.5, −0.5) and (0.5, 0.5, 0.5) out of those 15 runs of experiments and another point which was the theoretically optimal point (0.889794, 0.11886, 0.56201) related to the real value of the following process parameters: homogenization speed of 23,035.7 rpm, duration of 5.47544 min, and temperature of 75.6201°C, respectively. Considering the limitation of equipment and real situation, theoretically optimal point was checked under approximately 24,000 rpm of homogenization speed, approximately 5.5 min

of duration, and approximately 76°C of temperature. We performed these checkpoint analyses in triplicates to ensure reproducibility. These experiments were done to check if the experimental response values obtained were approximately the same as the theoretical response values calculated by the secondary equation.

RESULTS AND DISCUSSION

Influence of Process Parameters on Particle Size

Table II summarized the responses obtained with the Box–Behnken design for the average particle size (Y_1), the polydispersity index (PI), and the encapsulation efficiency (Y_2). It has been known that, during cubosomes preparation, temperature is crucial due in large part to the temperature-dependent phase behavior of the particles (8). These literatures cited in the introduction of this manuscript served as the basis for the selection of our factors and their level. Figure 1 also provided an electron micrograph of the cubosomes indicating the cubic structure. The amorphous blobs observed in this figure may be either cubosomes that melted under the high-energy beam of the TEM instrument, residual vesicles (since this was not a Cryo-TEM analysis), or both types of artifacts. Further, Cryo-TEM analysis will elucidate this matter. It is also known that while TEM analysis focuses on the observation of a selected sample field with few particles, for example for run #6, the DLS data shown in Table II were consistent with a monodisperse size distribution profile (raw data of cumulative percent of intensity *vs*. mean diameter not shown). The DLS allows examining a high number of particles suggesting that the observed amorphous blobs may be accidental or of low probability of occurrence at larger scale of particle number.

These data suggested that cubosomes were indeed formed with particle size ranging from 88.2 to 252.2 nm.

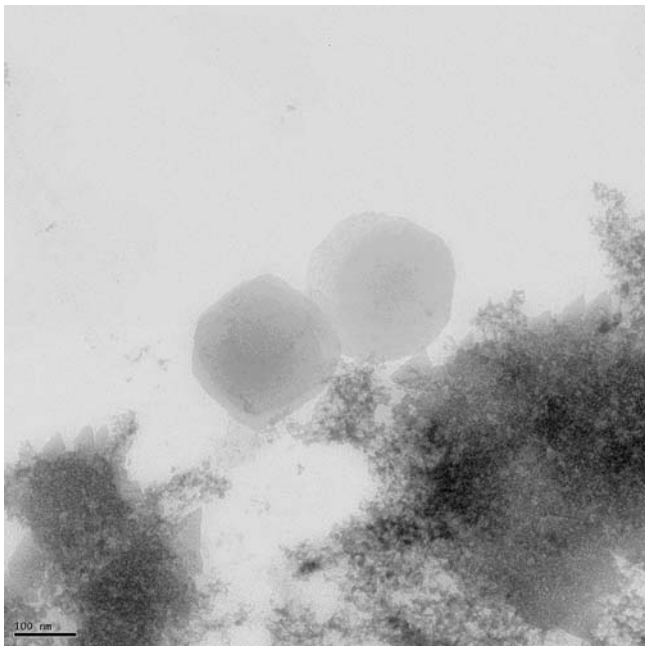

Fig. 1. TEM image of cubosome (run no. 6 in Table II) which shows the cubic structure of individual cubosome. *Scale bar* represents 100 nm

Table III. Observed and Predicted Values with Residuals of the Response Y_1

Run no.	Observed Y_1	Predicted Y_1	Residuals	% Error
1	107	112.3	−5.3	−4.7
2	93.9	83.3	10.6	12.7
3	107	123.3	−16.3	−13.2
4	144.9	144.0	0.9	0.6
5	106.8	107.7	−0.9	−0.8
6	252.2	244.3	7.9	3.2
7	96.5	104.4	−7.9	−7.6
8	149.2	146.5	2.7	1.8
9	200.8	199.0	1.8	0.9
10	112.9	115.6	−2.7	−2.3
11	110.6	100.9	9.7	9.6
12	123.0	112.3	10.7	9.5
13	139.9	150.5	−10.6	−7.0
14	163.7	173.4	−9.7	−5.6
15	88.2	90.0	−1.8	−2.0

These observations were further confirmed by X-ray diffraction analysis (data not shown). Because the method of Esposito (17) was adapted in this study with similar sample composition (nature and concentration) and preparation procedure, the current data are compared to those of the previous report. It appeared that the higher cubosome size range observed in this study was similar to that of Esposito *et al.* (17). However, relatively lower size was achieved in this study probably due to the use of higher homogenization speed. For example, in this study, speed range of 6,500 to 24,000 rpm was used while Esposito *et al.* (17) used a range of 500 to 1,500 rpm. It is noteworthy that the PI of the samples varied from to 0.005 to 0.191. According to NIST standards (27), almost half of the 15 runs were monodispersed while the other half was not. It was speculated that, in the polydispersed samples, there was a coexistence of cubosome with other vesicles as previously reported (5,17,28). It has been reported that, in order to produce colloidally stable cubic phase dispersions, the temperature should be in the range of

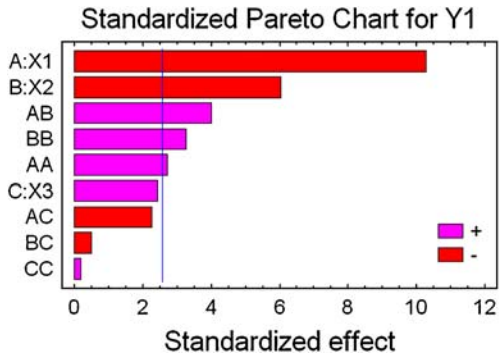

Fig. 2. Pareto chart shows the standardized effect of the independent variables and their interaction on Y_1 in initial (full) model. *Bars extending past the line* indicate values reaching statistical significance (α=0.05). *A* homogenization speed, *B* duration, *C* temperature, *AA* interaction of homogenization speed and homogenization speed, *BB* interaction of duration and duration, *CC* interaction of temperature and temperature, *AB* interaction of homogenization speed and duration, *AC* interaction of homogenization speed and temperature, *BC* interaction of duration and temperature

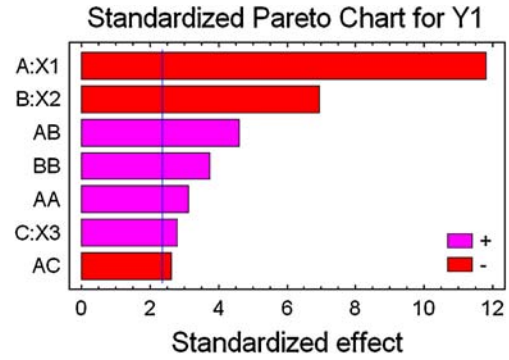

Fig. 3. Pareto chart shows the standardized effect of the independent variables and their interaction on Y_1 in reduced model. *Bars extending past the line* indicate values reaching statistical significance (α=0.05). Symbols are the same as in Fig. 2

40–80°C (8). All of our runs fitted into this category. Overall, the samples were milky emulsions in appearance. According to Table II, all the samples that have coded parameter X_1 of −1 had PI value of 0.005 (monodispersed) while most samples with X_1 of 1 had high PI value (up to 0.1901, polydispersed), which suggested that cubosomes were formed at relatively lower homogenization speed whereas at higher oscillatory frequency, perhaps cubic phases become highly elastic and highly viscous and small vesicles tend to agglomerate to a larger particle. All the samples with coded parameter X_2 of −1 had lower PI value (less than 0.021) while most of the samples with coded parameter X_2 of 1 had higher PI value (up to 0.187, polydispersed), which indicated that intermediate energy input helped the formation of cubosomes whereas overwhelming energy input helped the formation of small vesicles that tended to accumulate into larger particles.

Table III showed the observed and predicted values with residuals of response Y_1 particle size. The initial polynomial equation (full model) for particle size (Y_1) was:

$$Y_1 = 112.33 - 44.05X_1 - 25.88X_2 + 10.43X_3 + 24.25X_1X_2 - 13.8X_1X_3 - 3.05X_2X_3 + 17.18{X_1}^2 + 20.58{X_2}^2 + 1.18{X_3}^2 \quad (3)$$

where Y_1 was particle size and X_1, X_2, and X_3 represented homogenization speed, duration, and temperature, respectively.

The coefficient of determination (R^2) value of Eq. (3) was 0.974 (adj. R^2=0.927), indicating that the model fit the data very well. The Y_1 values in 15 runs ranged from 88.2 to 252.2 nm. The lack-of-fit test was insignificant (F=2.2043; df=2, 3; p=0.3272), indicating again that the model fit the data well. The regression model itself was significantly different than the null model at the 0.05 level (F=20.6942; df=5, 9; p=0.0019).

These data suggested that the increase in homogenization speed resulted in a decrease in the particle size. Medium duration would favor smaller particle size. In general, temperature did not result in a significant difference in particle size. However, relatively higher temperature gave out a relatively smaller particle size, perhaps due to a decrease in the viscosity of the dispersion medium.

The values on the x-axis of Pareto charts of Figs. 2 and 3 were the so-called standardized effects, which are in fact the t values, obtained in the statistical interpretation of each coefficient of the regression analysis defined in the above Eqs. (2) and (3). The standardized effects of the independent parameters and their interactions on the dependent parameter are shown in the Pareto chart (Fig. 2), which indicates the main effects of the independent parameters and interactions that will exert significant influence on the Y_1 value. The factors whose bars pass the line (p value equals to 0.05) indicate significance on the response value. According to the chart in Fig. 2, X_1, X_2, X_3, X_1X_2, X_1X_3, ${X_1}^2$, ${X_2}^2$ contributed more to Y_1 value, and X_2X_3 and ${X_3}^2$ contributed less, in prediction of Y_1. Hence, X_2X_3 and ${X_3}^2$ were omitted from the full model to obtain a reduced second-order polynomial equation (Eq. 4):

$$Y_1 = 113.06 - 44.05X_1 - 25.88X_2 + 10.43X_3 + 24.25X_1X_2 - 13.8X_1X_3 + 17.09{X_1}^2 + 20.49{X_2}^2 \quad (4)$$

The Pareto chart of reduced model is shown in Fig. 3. The R^2 value in the reduced equation was 0.972 (adj. R^2= 0.945). Although the secondary model fit the data better (its adjusted R^2 was slightly larger), the difference was statistically insignificant. The lack-of-fit test was insignificant (F=1.4219; df=2, 5; p=0.4619), indicating again that the model fit the data well. The regression model was significant (F=35.1642; df=7, 7; p<0.001). There was strong evidence for the validity of this model as well. A comparison of the full and reduced regression models indicated no significant difference in model fit to the data. Analysis of variance results are shown in Table IV. The calculated F (F_{CAL}) value (equals to 0.14) was less than the tabled value of F, which equals to 3.97 at α=0.05 (df_1=5 and df_2=7). Hence, it was concluded that the omitting X_2X_3 and ${X_3}^2$ terms did not significantly influence Y_1 values. Two Pareto charts were constructed (Figs. 2 and 3) to

Table IV. Results of ANOVA of Initial and Secondary Models for Y_1 of Cubosome Formulations

ANOVA	*df*	SS	MS	R^2 value	F value	p value
Regression						
A	9	27,376.84	3,041.87	0.974	20.69	0.002
B	7	27,334.46	3,904.92	0.972	35.16	<0.001
Residuals						
A	5	734.96 (C1)	146.99 (D1)			
B	7	777.34 (C2)	111.05			

Y_1 particle size, *A* initial (full) model, *B* secondary model; $F_{CAL} = [(C_2 - C_1)/N_{TO}]/D_1 = 0.14$, where N_{TO} is the number of terms omitted (having a p value more than 0.05)

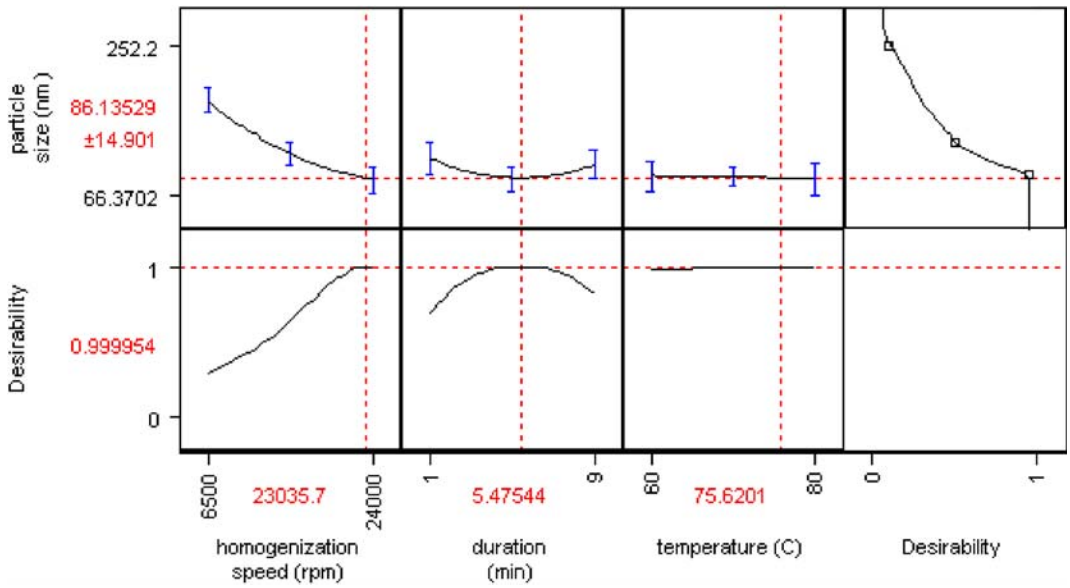

Fig. 4. Prediction and desirability plot of reduced model showing the effect of homogenization speed (X_1), duration (X_2), and temperature (X_3) on the particle size

compare the significance of factors before and after omission of the insignificant one.

Homogenization speed is related to shear rate, which is one strategy to provide energy input. As the cubosome's preparation process requires high energy (7), it is reasonable to increase the homogenization speed in order to reduce particle size. At relatively higher shear rate, cubic structure would be broken down to non-equilibrium vesicular structures which are more than likely to agglomerate into colloidally unstable larger particles (28). Duration is the homogenization time, which dictates the total energy input to the preparation process. The medium value of duration appears to be advantageous because prolonged duration would lead to cubosome destruction (28) and lower value will lead to failure of cubosome formation. With respect to temperature, a high value supplies more energy during the process and thus favors not only the formation of cubosomes but also the reduction in size (7). This is because appropriate heat provided in the preparation process will lead to improvement in the properties of the cubosomes (e.g., uniformity in size and morphology) and colloidal stability after the production phase (8–10). In our case, heat treatment turned the samples into milky dispersions with average diameter of 133 nm. This observation was consistent with previous literature (28). The reason lies in the transformation of larger vesicles into smaller cubosomes or L_2 phase particles, which is favored by heat (28). This can also occur by transport of molecular aggregation or dissociation mechanisms. However, the change in temperature did not lead to dramatic difference in size (Fig. 4). This could be explained by cloud point of polymer (Pluronic F127), which is beyond the temperature range in our case (60–80°C). The cloud point of Pluronic F127 is beyond 100°C (29). Therefore, in this study, the surface active property of the Pluronic remained stable over the temperature range studied. Considering that the cubosome dispersions are stabilized by Pluronic F127, very slow or even negligible fusion is expected below the cloud point (100°C). It is speculated that, beyond the cloud point of copolymer F127, the stabilization property of the surfactant would be altered leading to largely aggregated particles. But further experiment is needed to verify this hypothesis. There was strong evidence for the validity of the model as shown in Figs. 2 and 3.

The relationship between three-level, three-factor parameters and the response value, Y_1, in the reduced model was further investigated by constructing prediction and desirability plots. In Fig. 4, it was evident that higher levels of X_1 (homogenization speed) and X_3 (temperature) favored smaller Y_1 values of cubosomes while medium levels of X_2 (duration) favored the Y_1 values of cubosomes. This analysis was in agreement with previous studies (7) that reported cubosome preparation requires high-energy input.

Checkpoint Analysis

According to the reduced second-order polynomial equation (Eq. 4), three specific points (−0.5, −0.5, −0.5), (0.5, 0.5, 0.5), and (0.889794, 0.11886, 0.56201) were prepared and evaluated for Y_1, as shown in Table V. Results indicated that the measured Y_1 values were approximately the same as

Table V. Checkpoint Experiments Comparing Measured Predicted Y_1 value (n=3)

Run no.	X_1	X_2	X_3	Measured Y_1	Predicted Y_1	Error
C_1	−0.5	−0.5	−0.5	151.7±0.6	153.7	−4.3%
C_2	0.5	0.5	0.5	93.5±1.1	94.2	−0.7%
C_3	0.889794	0.11886	0.56201	88.4±1.3	85.6	3.3%

Table VI. Results of ANOVA of the Initial Model for Y_2 of Cubosome Formulations in Process Part

ANOVA	*df*	SS	MS	R^2 value	*F* value	*p* value
Regression Eq. (5)	9	0.0494	0.0055	0.76	0.2764	0.422
Residuals Eq. (5)	5	0.0993	0.0199			

Y_1 encapsulation efficiency

the predicted. The differences between the measured Y_1 values and predicted Y_1 values were found to be statistically insignificant: checkpoint C1: $t=-3.33$, $df=2$, $p=0.08$; checkpoint C2: $t=-0.64$, $df=2$, $p=0.59$; checkpoint C3: $t=2.15$, $df=2$, $p=0.16$. These results are additional evidence that the regression equation is an accurate model of the data.

Master Formula for Size Optimization

The optimum formulation would be one that would result in a low particle size, which falls into the category of 120–200 nm (30). Using a computer optimization process and the prediction and desirability plot shown in Fig. 4, we selected a level of 0.889794 for X_1, 0.11886 for X_2, and 0.5601 for X_3 (which was approximately 24,000 rpm of homogenization speed, 5.5 min of duration, and 76°C of temperature in real experiment). This optimal condition of process parameters for minimizing the particle size had a desirability ($d=$ 0.999954) which was very close to the ideal value of 1. The theory behind the ideal desirability value of 1 based on desirability function for simultaneous optimization of several response variables has been popularized by Derringer and Suich (31).

The theoretically optimal Y_1 value was 85.6 nm. For confirmation purposes, two fresh samples were prepared at the optimum levels of the independent parameters, and the resultant cubosome had an observed particle size of 88.4 nm (in Table V), which was in close agreement with the theoretical values.

Influence of Process Parameters on Encapsulation Efficiency

In this study, we investigated the optimization for process parameters. According to the statistical analysis, we found that the model fitted Y_1 very well ($R^2>0.90$) while the model had a lack of fitted for Y_2. The initial polynomial equation (full model) for encapsulation efficiency (Y_2) was:

$$Y_2 = 0.087 - 0.025X_1 - 0.031X_2 + 0.049X_3 - 0.065X_1X_2 + 0.029X_1X_3 - 0.036X_2X_3 + 0.073{X_1}^2 + 0.072{X_2}^2 + 0.046{X_3}^2 \quad (5)$$

According to Table VI, the R^2 value of the EE model is 0.76 (adj. $R^2=0.328$) much less than 0.90, which indicated that the model was not valid. Even when a Box Cox Y Transformation (32) was attempted on EE, the resulting R^2, which equaled to 0.79, was still less than 0.90. In this case, the current data set was not suitable for analysis and prediction with a multiple regression model. Table II showed that the highest encapsulation efficiency reached was 33.8%. Enhanced loading of negatively charged, water-soluble active ketoprofen by the inclusion of positively charged surfactants into cubosome formulation has been reported (11). And dacarbazine exhibits some water solubility. In future experiments, such electrostatic interaction-based approaches and comprehensive factors will be taken into account in order to explore a wider range of values for the independent parameters in order to better predict and enhance the EE.

CONCLUSION

This study demonstrated the use of a Box–Behnken design in optimizing the particle size (Y_1) of cubosomes in this investigation of the process parameter section. The derived polynomial equations and Pareto charts proved to be satisfactory in predicting Y_1 values for the preparation of optimal cubosomes with the desired particle size. In this study, minimal particle size would be achieved with approximately 24,000 rpm of homogenization speed, 5.5 min of duration, and 76°C of temperature (as process parameters), which resulted in cubosomes of 85.6 nm in size and 16.7% in encapsulation efficiency. Unfortunately, no valid model was found to predict the encapsulation efficiency with these data. Further experiments should be conducted to discover appropriate process parameters and formulation variables to increase the encapsulation efficiency without increasing particle size.

Acknowledgements

Monoolein was kindly provided to us by Danisco Cultor (Grindsted, Denmark). We also appreciated the guidance of Dr. Elizabet Kostoryz (Division of Pharmacology, University of Missouri—Kansas City) for the DLS experiment and the support of Randy Tindall (Electron Microscopy Center, University of Missouri—Columbia) for the electron microscopy.

REFERENCES

1. Luzzati V, Tardieu A, Gulik-Krzywicki T, Rivas E, Reiss-Husson F. Structure of the cubic phases of lipid–water systems. Nature. 1968;220(5166):485–8.
2. Scriven LE. Equilibrium bicontinuous structure. Nature. 1976;263:123–5.
3. Larsson K. Two cubic phases in monoolein–water system. Nature. 1983;304:664.
4. Shah JC, Sadhale Y, Chilukuri DM. Cubic phase gels as drug delivery systems. Adv Drug Deliv Rev. 2001;47(2–3):229–50.
5. Barauskas J, Johnsson M, Tiberg F. Self-assembled lipid superstructures: beyond vesicles and liposomes. Nano Lett. 2005;5 (8):1615–9.
6. Drummond CK, Fong C. Surfactant self-assembly objects as novel drug delivery vehicles. Curr Opin Colloid Interf Sci. 1999;4:8.
7. Garg G, Saraf S, Saraf S. Cubosomes: an overview. Biol Pharm Bull. 2007;30(2):350–3.
8. Worle G, Drechsler M, Koch MH, Siekmann B, Westesen K, Bunjes H. Influence of composition and preparation parameters on the properties of aqueous monoolein dispersions. Int J Pharm. 2007;329(1–2):150–7.
9. Worle G, Siekmann B, Bunjes H. Effect of drug loading on the transformation of vesicular into cubic nanoparticles during heat treatment of aqueous monoolein/poloxamer dispersions. Eur J Pharm Biopharm. 2006;63(2):128–33.
10. Worle G, Siekmann B, Koch MH, Bunjes H. Transformation of vesicular into cubic nanoparticles by autoclaving of aqueous

monoolein/poloxamer dispersions. Eur J Pharm Sci. 2006;27 (1):44–53.
11. Lynch ML, Ofori-Boateng A, Hippe A, Kochvar K, Spicer PT. Enhanced loading of water-soluble actives into bicontinuous cubic phase liquid crystals using cationic surfactants. J Colloid Interf Sci. 2003;260(2):404–13.
12. Hyde ST, Anderson S, Ericsson B, Larsson K. A cubic structure consisting of a lipid bilayer forming an infinite periodic minimum surface of the gyroid type in the glyceryl monooleate–water system. Z Kristallogr. 1984;168:213–9.
13. Nylander T, Mattisson C, Razumas V, Meizis Y, Hakansson B. A study of entrapped enzyme stability and substrate diffusion in a monoglyceride-based cubic liquid crystalline phase. Colloid Surf A: Physicochem Eng Aspects. 1996;114:311–20.
14. Engstrom S, Ericsson B, Landh T. A cubosome formulation for intravenous administration of somatostatin. Proc Int Symp Control Rel Bioact Mater. 1996;23:382–383.
15. Leesajakul W, Nakano M, Taniguchi A, Handa T. Interaction of cubosomes with plasma components resulting in the destabilization of cubosomes in plasma. Colloids Surf. 2004;34(4):253–8.
16. Norlen L. Nanostructure of the stratum corneum extracellular lipid matrix as observed by cryo-electron microscopy of vitreous skin sections. Int J Cosm Sci. 2007;29(5):335–52.
17. Esposito E, Eblovi N, Rasi S, Drechsler M, Di Gregorio GM, Menegatti E, *et al.* Lipid-based supramolecular systems for topical application: a preformulatory study. AAPS PharmSciTech. 2003;5(4):E30.
18. Spicer PT, Hayden KL, Lynch ML, Ofori-Boateng A, Burnes JL. Novel process for producing cubic liquid crystalline nanoparticles (cubosomes). Langmuir. 2001;17:5748–56.
19. Schadendorf D, Ugurel S, Schuler-Thurner B, Nestle FO, Enk A, Brocker EB, *et al.* Dacarbazine (DTIC) *versus* vaccination with autologous peptide-pulsed dendritic cells (DC) in first-line treatment of patients with metastatic melanoma: a randomized phase III trial of the DC study group of the DeCOG. Ann Oncol. 2006;17(4):563–70.
20. Bei D, Marszalek J, Youan BBC. Formulation of dacarbazine-loaded cubosomes—Part I: influence of formulation parameters. AAPS PharmSciTech. 2009; doi:10.1208/s12249-009-9293-3.
21. Trikalitis PN, Rangan KK, Bakas T, Kanatzidis MG. Single-crystal mesostructured semiconductors with cubic Ia3d symmetry and ion-exchange properties. J Am Chem Soc. 2002;124(41):12255–60.
22. Svensson O, Thuresson K, Arnebrant T. Interactions between drug delivery particles and mucin in solution and at interfaces. Langmuir. 2008;24(6):2573–9.
23. Solanki AB, Parikh JR, Parikh RH. Formulation and optimization of piroxicam proniosomes by 3-factor, 3-level Box–Behnken design. AAPS PharmSciTech. 2007;8(4):E86.
24. Maghsoudi A, Shojaosadati SA, Vasheghani Farahani E. 5hFluorouracil-loaded BSA nanoparticles: formulation optimization and *in vitro* release study. AAPS PharmSciTech. 2008;9(4):1092–6.
25. Nattapulwat N, Purkkao N, Suwithayapan O. Preparation and application of carboxymethyl yam (*Dioscorea esculenta*) starch. AAPS PharmSciTech. 2009;10(1):193–8.
26. Box GEP, Behnken DW. Some new three level designs for the study of quantitative variables. Technometrics. 1960;2:455–76.
27. Hackley VA, Ferraris CF. The use of nomenclature in dispersion science and technology. NIST Recommended Practice Guide. Special Publication. 2001;960(3):76.
28. Barauskas J, Johnsson M, Joabsson F, Tiberg F. Cubic phase nanoparticles (cubosome): principles for controlling size, structure, and stability. Langmuir. 2005;21(6):2569–77.
29. Christiansen C, Muller BW. Cloud point temperature measurement methods for surfactant characterization. Pharm Ind. 2002;64:278–82.
30. Moghimi SM, Hunter AC, Murray JC. Long-circulating and target-specific nanoparticles: theory to practice. Pharmacol Rev. 2001;53(2):283–318.
31. Derringer G, Suich R. Simultaneous optimization of several responses variables. J Qual Technol. 1980;12:214–9.
32. Box GEP, Cox DR. An analysis of transformations. J Royal Stat Soc B. 1964;26:211–43.